HIGH HEAT FLUX MEASUREMENTS AND EXPERIMENTAL CALIBRATIONS/CHARACTERIZATIONS*

*C. T. Kidd***
Calspan Corporation/AEDC Operations
Arnold Engineering Development Center
Arnold Air Force Base, Tennessee 37389

ABSTRACT

Recent progress in techniques employed in the measurement of very high heat-transfer rates in reentry-type facilities at the Arnold Engineering Development Center (AEDC) is described. These advances include thermal analyses applied to transducer concepts used to make these measurements; improved heat-flux sensor fabrication methods, equipment, and procedures for determining the experimental time response of individual sensors; performance of absolute heat-flux calibrations at levels above 2,000 Btu/ft^2-sec (2.27 kW/cm^2); and innovative methods of performing in-situ run-to-run characterizations of heat-flux probes installed in the test facility. Graphical illustrations of the results of extensive thermal analyses of the null-point calorimeter and coaxial surface thermocouple concepts with application to measurements in aerothermal test environments are presented. Results of time response experiments and absolute calibrations of null-point calorimeters and coaxial thermocouples performed in the laboratory at intermediate to high heat-flux levels are shown. Typical AEDC high-enthalpy arc heater heat-flux data recently obtained with a Calspan-fabricated null-point calorimeter installed in a generic flow-field probe model are included.

NOMENCLATURE

a	Radius of null-point cavity, in.
b	Distance from front surface of null-point calorimeter to the null-point cavity, in.
C_p	Specific heat capacity, Btu/lb-°F
d	Diameter of null-point cavity, in.
K	Thermal conductivity, Btu/in.-sec- °F
k	Thermal diffusivity, in.^{2}/sec
L	Length of null-point calorimeter, in.
ℓ	Distance from top surface of semi-infinite solid, or thickness of finite thickness slab, in.
$\dot{q}$	Calculated or measured heat flux or heat-transfer rate, Btu/ft^2-sec
$\dot{q}_o$	Constant heat flux or heat-transfer rate, Btu/ft^2-sec
R	Radial distance from axial centerline of TRAX analytical model, in.
r	Radial distance from axial centerline of null-point cavity, in.
T	Temperature, °F
T_b	Temperature on axial centerline of null point, °F
T_s	Temperature on surface of null-point calorimeter, °F
t	Time, sec
x	Distance in axial direction from bottom surface of finite thickness slab, in.
Z	Distance in axial direction of TRAX analytical model, in.
ρ	Density, lb/in.^{3}

Subscripts

b	At null-point surface
s	Surface conditions
o	Initial conditions

INTRODUCTION

Recent national test programs such as the National Aero-Space Plane (NASP) have demonstrated the requirement to measure very high heat flux, possibly as high as 80,000 Btu/ft^2-sec (90.8 kW/cm^2). Aerospace simulation facilities such as high-enthalpy arc-driven wind tunnels have been used to produce reentry-type aerothermal test environments.

* The research reported herein was performed by the Arnold Engineering Development Center (AEDC), Air Force Systems Command. Work and analysis for this research were done by personnel of Calspan Corporation/AEDC Operation, operating contractor for the AEDC aerospace flight dynamics facilities. Further reproduction is authorized to satisfy needs of the U. S. Government.

** Principal Engineer, Member ISA.

Probably the most important parameter to be considered in reentry is the stagnation point aerodynamic heating rate. Heat flux in these facilities can exceed 25,000 Btu/ft^2-sec (28.4 kW/cm^2) and pressures can reach 160 atm. The experimental determination of these heat-flux levels has always presented a difficult challenge to the measurement engineer. Measurement of heat flux at the stagnation position of simple test model configurations (usually sphere cones) is required to determine the facility flow conditions, since stagnation temperature measurements are not possible with conventional intrusive probes because of the extremely high temperatures (7,500° F) in the flow field. The test environment is usually so harsh that very few of the commonly used discrete heat-flux transducers can survive even short exposures in the test medium. Even the more rugged sensors often experience surface ablation before a meaningful measurement can be made. Exposure times of 50 to 100 msec are typical. This leaves the measurement engineer few practical choices in the development of an effective transducer for this application.

The transducer most commonly used to measure high heat-flux levels in high pressure, arc-heated flow-field environments is the null-point calorimeter.[1-4] Other devices such as coaxial surface thermocouples,[5-8] Gardon gages,[9] and slug calorimeters[10] have been used with varying degrees of success. Each of these has shortcomings which limit their effectiveness in this measurement application. The null-point concept has been used extensively in this application because of its relatively simple principle of operation, adequate time response, and time to burnout. In 1977 the American Society for Testing and Materials (ASTM) officially adopted the null-point calorimeter as a "Standard Method for Measuring" in this application and reapproved this method in 1990.[11] The first application of the null-point calorimeter in an arc-heated flow field involved installing the device in the stagnation position of a probe model such as a sphere-cone and locating the probe on the axial centerline of an arc jet.[2] The nosetip was often protected by a Teflon® cap which was ablated away in a fraction of a second after the arc was ignited. This method had several obvious deficiencies which included the following:

1. Measurements were made at only one location in the flow field;

2. The probe could only be used for one run because of severe nosetip ablation and ultimate destruction; and

3. Significant differences in the indicated heat-flux levels from different null-point calorimeters were commonplace.

As early as 1971, Kennedy, et al.,[3] began using a swept technique for heat-transfer measurements in the Acurex/Aerotherm arc facility. This technique involved installing one or more null-point probe models on a rake and sweeping them through the arc-heated flow field at a rate slow enough to allow the sensor to make accurate measurements, yet fast enough to prevent model ablation. This method has the advantages of measuring the heat-flux profile across the entire jet and preserving the probe/sensor for repeated measurements. Nearly every arc facility making heat-flux measurements with null-point calorimeters has adopted the swept probe method.

Although used by many experimenters and having been developed a relatively long time, the operating principles and the effects of variations in physical dimensions are not well understood in the aerothermodynamic test community. This paper provides comprehensive thermal analyses of the null-point calorimeter concept with emphasis on the effects of variations in the physical dimensions. Some of the common prevailing perceptions about null-point calorimeters are shown to be incorrect. Laboratory experimental data which complement the thermal analyses are shown.

A common misconception prevalent among null-point calorimeter users and suppliers is that it is not possible to provide meaningful experimental time response and calibration data at heat-flux levels close to the measured values in the laboratory. There are only two known commercial sources of null-point sensors, and neither provides meaningful transient time response or calibration data. Since the time response of null-point calorimeters is marginal for arc facility heat-flux measurement applications, an experimental determination of this parameter is essential for accurate measurements. Methods have been developed at the AEDC to provide these data on a routine basis in the laboratory. The experimental apparatus/system which was developed to provide these data is described in this paper and graphical illustrations of typical experimental data are also included.

A unique method of providing run-to-run calibrations and characterizations of null-point sensors in the test area through the facility data acquisition and processing system has been developed and implemented. Experimental data from this system are also included in this paper.

Another sensor extensively used in high heat-flux measurement applications is the Chromel®-constantan coaxial surface thermocouple. Although the coaxial thermocouple has very fast time response,

excellent durability, and contourability, this sensor has one limiting factor which precludes its use in very high heat-flux measurement applications. The value of the lumped thermal parameter of interest (primarily thermal conductivity) of Chromel and constantan is only about 20 percent that of copper. This causes the surface temperature of the coaxial thermocouple to rise almost five times faster than a copper null-point sensor. This is a detriment in very high heat-flux measurement applications because of its shorter time to burnout (ablation). However, the Chromel-constantan sensor can be used in slightly higher (≈2,200°F) temperature environments than copper (≈2,000°F) materials. Chromel-constantan sensors can normally be used in applications involving stainless steel materials.

In the aerothermodynamic test community, increasing demands are being made to obtain more heat-transfer data in each succeeding wind tunnel test. Normally, these are low to intermediate (< 1,000 Btu/ft^2-sec) measurement applications. This often translates into leaving the test article in the tunnel flow for longer periods of time. As a result of this practice, surface temperature data are obtained with coaxial surface thermocouples for periods of time which exceed the limits defined by semi-infinite solid restrictions. Therefore, another method of data processing must be used. One of these is a one-dimensional finite difference heat conduction code developed by E.O. Marchand[12] for calculations on a finite length body. This heat conduction code is being investigated at the AEDC as a possible replacement for the semi-infinite equations under appropriate test conditions. This paper contains limited results of analytical evaluations of the finite difference code in heat-transfer measurement applications.

NULL-POINT CONCEPT

Figure 1 is a sketch of the null-point concept of heat-flux measurement. The sketch is a physical illustration of a thermal mass of length L with a flat bottom cylindrical hole of radius a drilled from the backside of the mass to within a distance b of the front surface. The location 0, b on the radial centerline of the cylindrical cavity is defined as the null point. A transient backside temperature T_b, (0, b, t) measured at the null point is assumed to be identical to the surface temperature history T_s (r, o, t) on the outside surface of the same thermal mass in the absence of the cavity. Therefore,

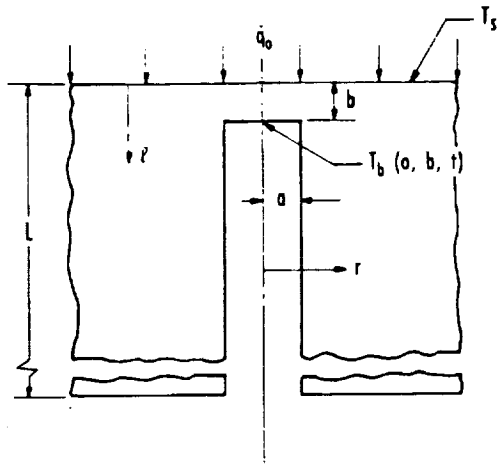

Fig. 1. Concept sketch of null-point calorimeter.

the temperature history measured at the null point could be inserted into a one-dimensional inverse heat conduction equation for a semi-infinite solid to determine the heat-transfer rate at the surface of the solid.

PRACTICAL IMPLEMENTATION OF CONCEPT

A section view sketch of a null-point calorimeter showing all important components and the physical configuration of the sensor is shown in Fig. 2. The outside diameter is 0.093 in., the length is 0.40 in., and the body material is oxygen-free high conductivity (OFHC) copper. Temperature at the null point is measured by a 0.020-in.-diam ANSI type K stainless steel-sheathed thermocouple with 0.004-in.-diam thermoelements. Although no thermocouple attachment is shown, it is assumed that the individual thermocouple wires are in perfect contact with the backside of the cavity and present no added thermal mass to the system. Note that the null-point body has

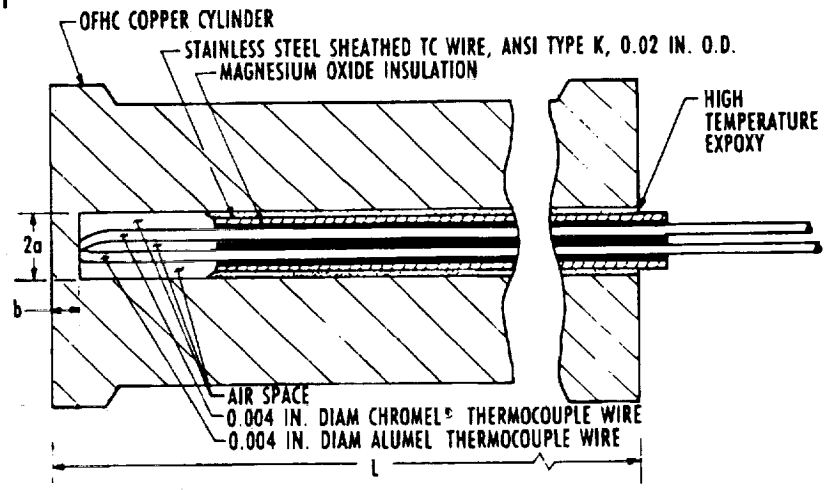

Fig. 2. Section view of null-point calorimeter assembly no scale.

a slight chamfer at the top and bottom which creates an effective circumferential dead air space along the length of the cylinder to enhance one-dimensional heat conduction and prevent radial heat conduction. For aerodynamic heat-transfer measurements, the null-point sensors are generally pressed into the stagnation position of a sphere cone model.

THERMAL ANALYSIS

Results of thermal analyses presented in this paper were obtained with a finite-element heat conduction code called TRAX[13] which is used to perform transient analyses on axisymmetric bodies. Many heat-transfer problems can be geometrically configured by axisymmetric bodies, thus providing the capability for performing the analyses in three dimensions. This analytical method is practically implemented by designing a plane geometry matrix which simulates the aerodynamic configuration of interest, consisting of a number of finite elements. These elements are usually, but not exclusively, rectangles with nodal points specified at each of the four corners. Constant heat flux, heat-transfer coefficient, and temperature boundary conditions can be specified between any two nodal points on the analytical model. Different time steps can be specified in the same problem, and different boundary conditions and thermal properties may be specified for each time interval. A tabulated temperature history at each nodal point on the analytical model is provided by the TRAX computer program.

The finite-element model used to represent the null-point calorimeter in this paper is shown by the block diagram in Fig. 3. This geometry has 793 finite elements and 879 nodal points. This block diagram sketch is not to scale. Finite-element numbers are shown within the blocks and nodal point numbers are shown on the sides of the blocks. Because of space limitations and clarity in presentation, only a small number of the finite elements, nodal points, and dimensions are illustrated on the block diagram in Fig. 3. The axisymmetric model is achieved by rotating the plane geometry sketch around the axial centerline shown on the left-hand side of the sketch. Note the "open window" beginning with nodal points 313 to 315 near the top of the model and ending with nodal points 807 to 809. This window represents the circumferential dead air space on a null-point calorimeter installation. All material to the right side of the air space is considered to be model material, also OFHC copper. The physical dimensions of the null-point cavity shown in Fig. 3 are considered by

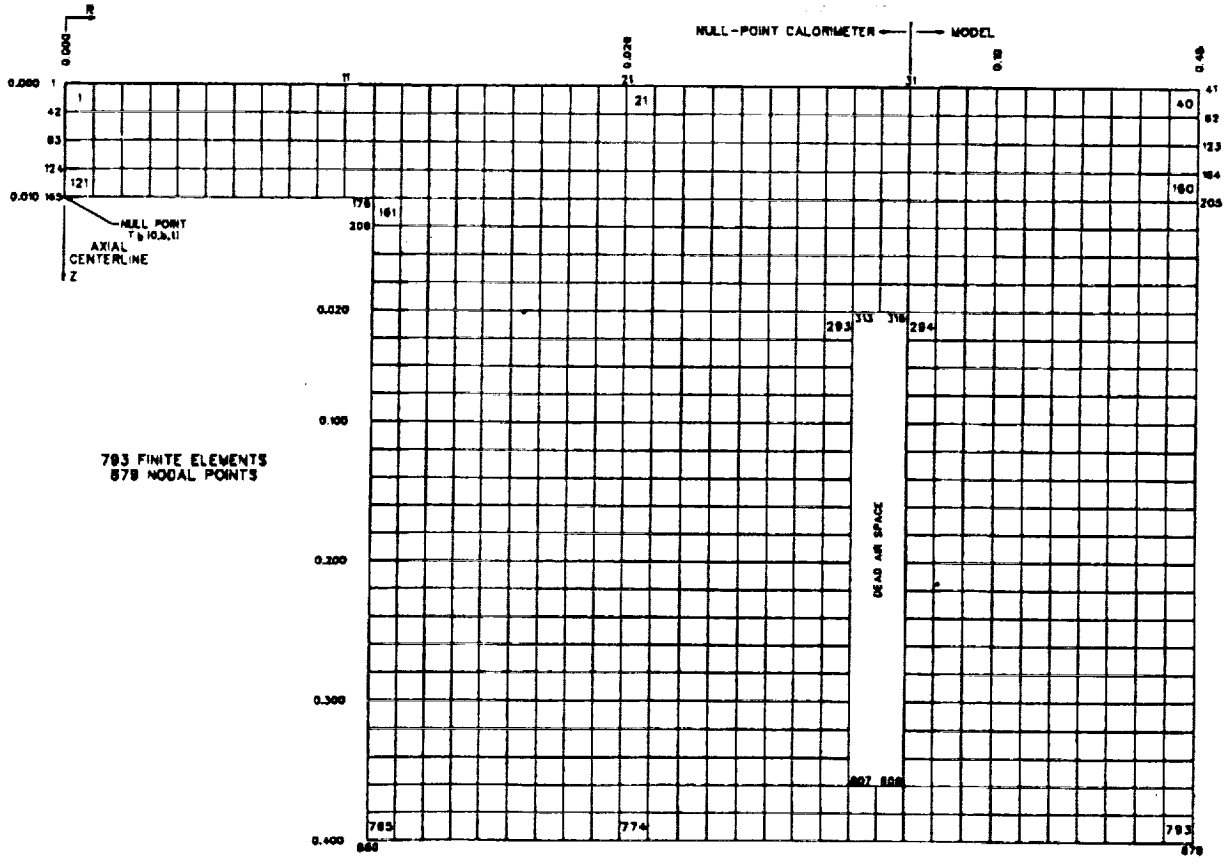

Fig. 3. TRAX model of null-point calorimeter.

some[2,11] to be the ideal geometry with the parameter a/b = 1.1 (a = 0 .011 in. and b = 0.10 in.). Note the dimensions shown on the perimeter of the sketch. These dimensions are frequently changed to show the effects of geometrical changes.

Effects of Changes in Dimensional Parameters — According to the majority of analysts and/or experimenters quoted in the open literature,[2, 3, 11] the optimum value of the ratio of null-point calorimeter cylindrical cavity radius a to the copper thickness above the cavity is stated to be between 1.0 and 1.1. Analytical results presented in this paper do not support that position. First, a statement defining the term "optimum" with regard to the performance of the sensor is needed. An optimum value of the parameter a/b is defined as a value which yields the fastest time response to a step heat-flux input and maintains a constant value of indicated $\dot{q}$/input $\dot{q}$ ($\dot{q}/\dot{q}_o$) after the initial time response period. The analytical results do not necessarily have to give a value of $\dot{q}/\dot{q}_o$ = 1.0, since this difference can be experimentally calibrated in the laboratory.

Figures 4 and 5 show analytical time response data for several null-point calorimeter geometries. In both illustrations, the radius a of the cylindrical cavity is held constant and the thickness b of the copper above the cavity is varied. A timewise temperature history T(t) at the back centerline nodal point (#165, see Fig. 3) was calculated by the TRAX program. Data were computed at 0.0002-sec intervals. The timewise temperature history at this nodal point was input to the numerically represented one-dimensional inverse heat conduction equation shown as Eq. (1),

$$\dot{q}(t) = \frac{2(\rho C_p K)^{\frac{1}{2}}}{\pi^{\frac{1}{2}}} \left[\sum_{i=1}^{n} \frac{T_i - T_{i-1}}{(t_n - t_i)^{\frac{1}{2}} + (t_n - t_{i-1})^{\frac{1}{2}}} \right] \quad (1)$$

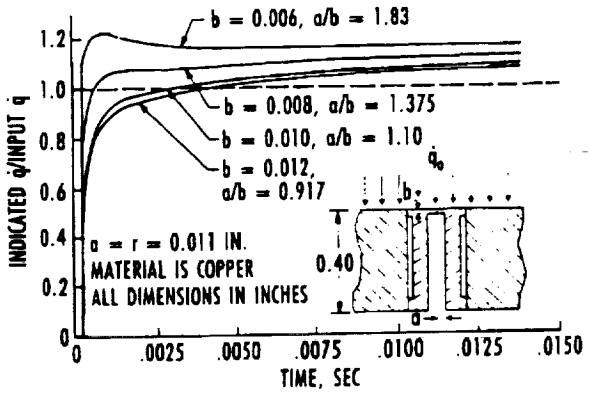

Fig. 4. Null-point calorimeter analytical time response data.

where ρ, C_p, and K are the density, specific heat, and thermal conductivity, respectively, of the OFHC copper casing. Equation 1 is a short-form version of the Cook and Felderman equation[14] developed by Don Wagner of Sverdrup Technology in 1974. Figure 4 illustrates the time response of a null-point calorimeter of radius a = 0.011 in. as the copper thickness b is varied from 0.006 to 0.012 in. in 0.002-in. increments. This resulted in a variation in a/b from 1.83 to 0.917. From the data illustrated on Fig. 4, it is apparent that the greater thicknesses generally result in slower time responses. It is also apparent that the indicated $\dot{q}$/input $\dot{q}$ ($\dot{q}/\dot{q}_o$) asymptotes are above 1.0 even for the lower values of a/b. The illustration of the case for a/b = 1.375 (b = 0.008 in.) seems to be optimum in that the time to 95 percent of full scale is reached in less than 1 msec and the asymptote for $\dot{q}/\dot{q}_o$ approaches 1.1. The case for a/b = 1.83 (b = 0.006 in.) results in a 23-percent overshoot of $\dot{q}/\dot{q}_o$, tapering down to an asymptote of 1.15. Even though a fast response is realized with this configuration, the overshoot should be avoided, since it indicates an unrealistic value of $\dot{q}/\dot{q}_o$ at the beginning of the process. Although not illustrated as in this paper, this type of overshoot has been reported by other analysts.[2]

Figure 5 is an illustration of null-point calorimeter time response data when the radius is held constant at a value of a = 0.00825 in. and the thickness b is allowed to vary from 0.002 to 0.010 in. The optimum value of a/b shown on Fig. 5 occurs at the same a/b ratio as it did on Fig. 4; i.e., a/b = 1.375. When the value of a/b was increased to 4.0, as shown on Fig. 5, this produced a very high value of $\dot{q}/\dot{q}_o$ early in the run time. This thermophysical phenomenon is caused by a thin copper foil above the null-point cavity. This type of overshoot has been observed with a small number of commercial units in laboratory experiments and in units fabricated by Calspan to intentionally

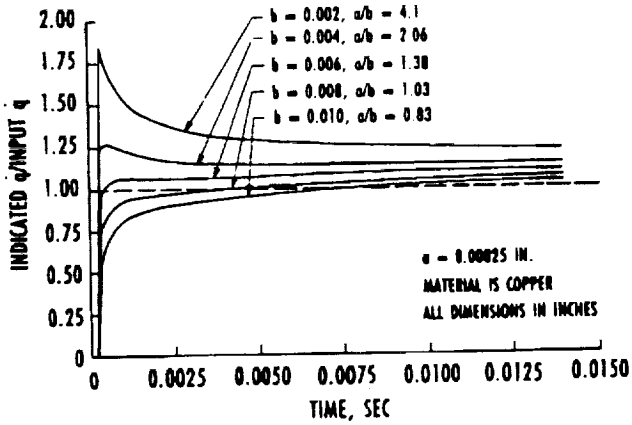

Fig. 5. Null-point calorimeter analytical time response data.

exhibit this type of behavior. Laboratory experimental data which show this effect are presented in the Experimental Considerations section.

Based primarily on a time response criterion, it appears from the analytical data presented in this paper the optimum value of the ratio of the cylindrical cavity radius to the thickness above the cavity (a/b) is 1.375. This value is slightly higher than reported by other analysts.

Effect of Locating the Temperature Sensor Off the Axial Centerline — The data obtained from thermal analyses performed on the null-point concept shown to this point assume that the temperature sensor was located on the axial centerline of the cylindrical cavity. This section is concerned with the effect of locating the temperature sensor off the axial centerline. Figure 6 shows that placement of the temperature sensor at a location of up to $r_o/a = 0.5$ will cause an error of less than 3 percent. This result is usually acceptable and adds credibility to the null-point concept in that a strict centerline location of the thermoelements is not essential to obtain high-quality data.

Effective Run Time — Effective run time is an important parameter when the null-point calorimeter is used for heat-flux measurements. Since the inverse heat conduction relationship for a semi-infinite solid is used to obtain data from the null-point sensor, the semi-infinite solid limitations apply in data processing. These limitations primarily involve the length of the null-point calorimeter and the time over which data are to be obtained. An exact temperature history calculated from the relationship for a solid of finite length[15] was inserted into the numerical heat-flux solution for a semi-infinite solid to produce the normalized error curve shown in Fig. 7. This relationship was developed by the author and has been reproduced by others.[6, 7] Figure 7 illustrates that the following relationship [Eq. (2)] must be true to ensure that the error in indicated heat flux does not exceed one percent:

$$\frac{L}{(kt)^{1/2}} \leq 1.8 \qquad (2)$$

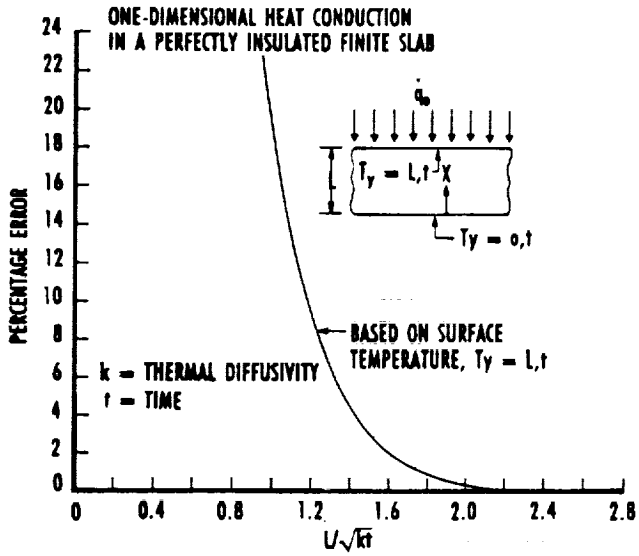

Fig. 7. Errors in indicated heat transfer rate incurred by assuming semi-infinite solid behavior for a finite length slab.

where L is transducer length, k is thermal diffusivity, and t is time from initial heating. For a copper null-point calorimeter of length, L = 0.4 in., the effective run time is 0.28 sec. This result is substantiated by the TRAX heat conduction code as shown in Fig. 8. Although the normalized value of indicated $\dot{q}$/input $\dot{q}$ is 1.07 rather than 1.0, the reader can see that the value reaches 1.08 in less than 0.30 sec.

Effects of Variations of Thermal Properties with Temperature — The value of the lumped thermal parameter of copper is not a strong function of temperature. In fact, the value of $(\rho CpK)^{1/2}$ of OFHC copper increases only 5 percent over 1,000°F.[16] Thermal properties of OFHC copper are well documented and data from different sources are in good agreement. Because the $(\rho CpK)^{1/2}$ parameter of copper is relatively constant over a wide temperature range, most experimenters use the room temperature value of the parameter in processing data from null-point calorimeters. However, the variation in the lumped thermal parameter, as obtained from reliable handbook data, can easily be programmed into appropriate data processing relationships.

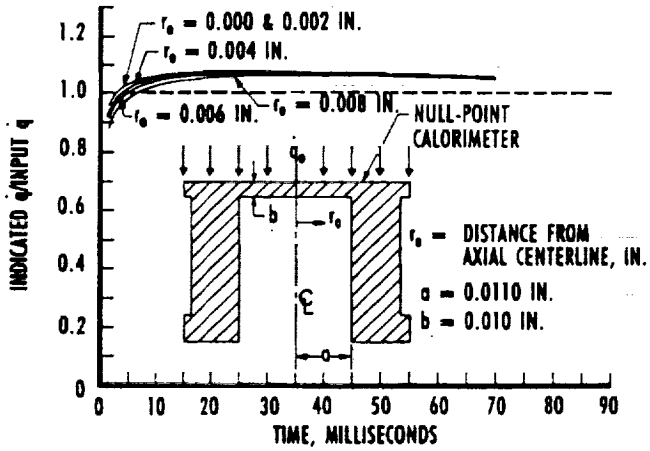

Fig 6. Effect of locating temperature sensor off axial centerline.

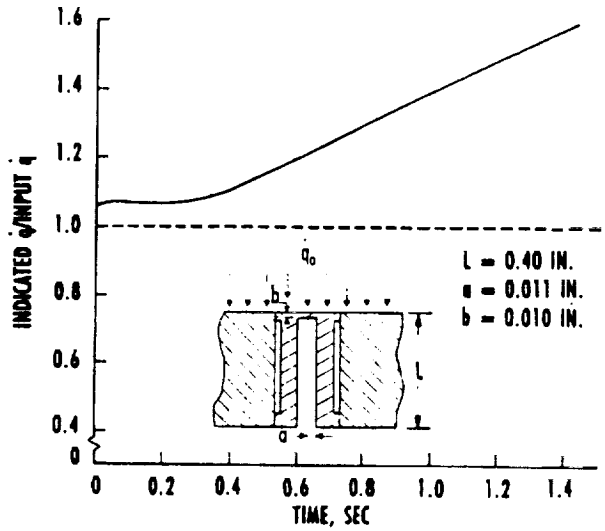

Fig. 8. Effect of heating null-point calorimeter past semi-infinite solid run time.

COAXIAL SURFACE THEROMOCOUPLE

DESCRIPTION

A coaxial surface thermocouple begins with a small diameter thermoelement wire coated with a thin (≤ 0.0005 in.) layer of special ceramic insulation (usually MgO) which is capable of withstanding temperatures up to 3,000°F. This inner wire with insulation is swaged into an outer tube of another compatible thermoelement material. The final assembly is effected by drawing the three-component unit (wire, insulation, and tube) down from an initial outside diameter of about 0.125 in. to a final diameter as small as 0.015 in. The coaxial thermocouple assembly is completed by attaching thermocouple lead wires to the coaxial thermoelements and slipping a transition fitting with high-temperature potting over the lead wires. This operation requires special equipment and "hands-on" experience. This applies to thermocouple materials, body length and diameter, lead wires, and transition fitting. Finally, the hot junction is completed by abrading the center conductor and outer tube together with #180 grit emery paper. A sketch of the coaxial thermocouple installation purchased commercially and used at the AEDC is shown in Fig. 9.

The principle of operation of the coaxial surface thermocouple[6,7,8] is similar to that of the null-point calorimeter. In fact, the primary difference is that with the null-point calorimeter an assumption is made that the measured temperature history is the surface temperature; whereas, with the coaxial surface thermocouple, this is a fact. A normal qualifying assumption with the coax TC is that the entire assembly behaves as a homogeneous, semi-infinite solid. This includes the model material as well as the

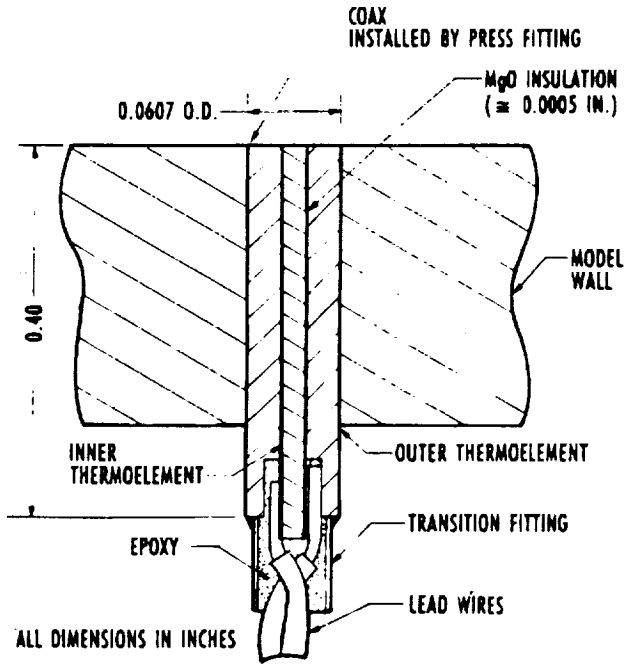

Fig. 9. Sketch of coaxial surface thermocouple installation.

thermoelements. The equation normally used to extract timewise heat-flux data from the coaxial thermocouple was shown earlier in this paper as Eq. 1.

Recently, a finite difference heat conduction code[12] has been used at the AEDC to obtain accurate timewise heat-flux data well beyond the time constraints of semi-infinite solid theory. This analytical code will be briefly described in the next section of this paper. Obviously, [from Eq. (1)] a close match of the lumped thermal parameter $(\rho CpK)^{1/2}$ of the thermoelements is necessary so that an analytical scale factor can be assumed for these sensors. Fortunately, there is a commonly used thermocouple pair whose thermoelements have $(\rho CpK)^{1/2}$ parameters which, at room-temperature, ambient conditions, are within 1 percent of the same value (see Table 1).

Table 1. Lumped Thermal Property Data for coaxial theromocouple and model materials.

MATERIAL	$(\rho CpK)^{1/2}$, Btu/ft^2-sec$^{1/2}$-°F
CHROMEL	0.410*
CONSTANTAN	0.408
300 SERIES STAINLESS STEEL	0.396

* ALL DATA OBTAINED AT ROOM TEMPERATURE AMBIENT CONDITIONS.

This thermocouple pair is Chromel-constantan (ANSI type E), which also has a higher thermoelectric sensitivity than any of the common thermocouples.[6] Another requirement is that the model or heat sinking material also have a lumped thermal parameter which matches that of the coaxial sensor materials. This requirement is not hard to satisfy in the majority of cases. Most of the 300-series stainless steels and 17-4 stainless have a lumped thermal parameter less than 10-percent different than the Chromel-constantan coaxial thermocouple. These facts make the coaxial surface thermocouple installed in stainless models a good choice for fast-response wind tunnel measurements.

DESCRIPTION OF FINITE DIFFERENCE COMPUTER CODE

In the majority of measurement applications involving coaxial surface thermocouples as heat-flux sensors, the transient surface temperature can be input to one of several short-form versions of the well-known numerical integration equation[14] to obtain the timewise heat flux. This numerical equation was developed to apply to transient heat conduction in solid bodies which qualify as semi-infinite in length over the time period of interest. Use of the semi-infinite solid equation is limited to the thermal penetration time defined by Eq. (2) given in a previous section of this paper. To obtain accurate heat-flux data beyond these time constraints, another method of data processing must be used. The method used at the AEDC is a finite difference technique developed by E. O. Marchand[12] for treating transient heat conduction problems in one space dimension. The computer code developed by Marchand employs a fully implicit, finite difference method for heat conduction within a planar body. The finite wall solution has no time limitations inherent in the methodology, but is somewhat more complex mathematically and requires careful analysis of each problem to ensure accurate results.

A computer program which incorporates the finite difference methodology was written to calculate surface heat flux from coaxial surface thermocouple timewise temperature data. This program is quite versatile in its ability to accept a number of nodal points which divide the finite wall into equal segments in the space dimension, and it allows control of the time integration steps. Several test problems which have exact mathematical solutions have been solved with the finite difference computer code with excellent results. Use of this code in this paper will be limited to one analytical problem for demonstration purposes only. For a more thorough use of the code in a variety of analytical and experimental applications, refer to Refs. 8 and 12.

THERMAL ANALYSIS OF THE COAXIAL SURFACE THERMOCOUPLE

The first step in the analysis procedure is to construct a finite-element model of the coaxial surface thermocouple system. A computer-generated block diagram of the coaxial surface thermocouple system (including model wall) is shown in Fig. 10. This is an axisymmetric scale model, but the scale is different in the axial and radial planes. The model is defined by 472 finite elements and 523 nodal points. Because of space limitations, only a few of the nodal points and finite elements are shown on the block diagram. Most of the finite elements are shown within the blocks, and the nodal points are shown on the edges of the blocks.

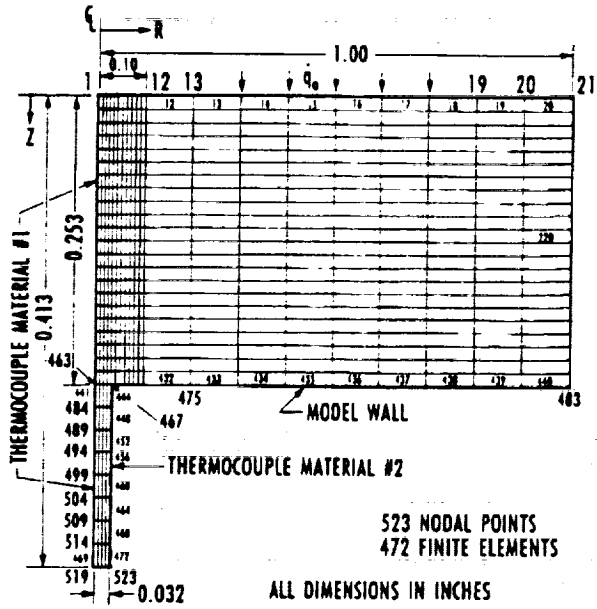

Fig. 10. Trax model of coaxial surface thermocouple system.

TRAX analytical model dimensions can be changed to illustrate the effects of varying the physical configuration of the coaxial TC system. The case for the length of the coaxial sensor being equal to the model wall thickness is accomplished by merely removing finite elements 441-472 (see Fig. 10). The analytical data presented were obtained with a constant and equal heat flux being applied at each nodal point on the top surface of the coaxial TC system (nodal points 1-21). Although the TRAX analytical model shown in Fig. 10 was constructed as a three-material system, all materials were assumed to have the same thermal properties (Chromel) to

eliminate the effects of different material properties from the results shown in this study.

Analytical Data — Figure 11 is a graphical illustration of the coaxial TC analytical data to be considered in this documentation. The overall system diameter (model and coaxial sensor) is 2.0 in. The coaxial wire diameter is 0.064 in., which closely approximates the actual commercial coaxial sensor diameter of 0.0607 in. presently used at the AEDC. The model wall thickness for all cases shown on Fig. 11 is 0.253 in. and the coaxial wire length is 0.413 in. This is an ideal example to illustrate the objective of this documentation. The length of the commercial coaxial surface thermocouples presently being purchased is about 0.40 in. Normally, the desired wall thickness is at least 0.375 in., but some model walls are closer to 0.250 in. With an input heat flux of 1.0 Btu/ft^2-sec applied between each nodal point on the model surface and considering adiabatic boundary conditions on all other surfaces, a transient temperature history was generated at 0.10-sec intervals at each nodal point on the TRAX model over a total time period of 10 sec. The TRAX temperature history at nodal point #1 was input to the normal semi-infinite solid data reduction equation [Eq. (1)] shown in a previous section of this paper. The resulting normalized timewise data are shown on the upper curve on Fig. 11. Obviously, using the semi-infinite solid equation for a finite thickness slab yields significant errors (+27 percent in indicated heat flux at a time duration of 8 sec). Of course, these data are consistent with the predicted errors shown on Fig. 7.

The same temperature history was input to Marchand's one-dimensional finite difference code. This code was formulated with ten nodes and 0.10-sec integration time steps. These results are shown by the lower curve on Fig. 11. The normalized timewise data (Indicated Heat Flux/Input Heat Flux) showed a consistent and negligible error through the entire run time of 10 sec. For a much more extensive analytical treatment of this problem, including effects of physical dimensional changes and longer run times, refer to Ref. 8.

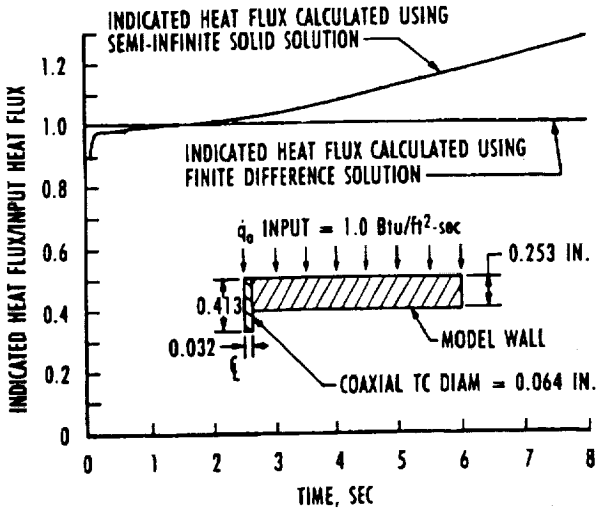

Fig. 11. Timewise coaxial to heat-flux data obtained with different data reduction methods.

FABRICATION

Although the design of null-point calorimeters and coaxial surface thermocouples is relatively simple with the aid of modern analytical heat conduction codes, the practical implementation of these designs, i.e., fabrication, has always been and remains a difficult task.

NULL-POINT CALORIMETERS

At the time of this writing, there are only two known commercial sources of null-point calorimeters, although there used to be at least four sources. Reasons for the decline of commercial null-point sensor vendors include the following:

1. there is not a high-volume demand for these sensors at this time,

2. the fabrication process used by the commercial vendors is difficult to control,

3. none of the commercial sources had an experimental facility in which the important performance parameters—primarily time response and calibration—could be determined, and

4. reliability of completed sensors was poor.

All commercial sources of null-point calorimeters use the same basic fabrication technique. The components and construction details of a null-point calorimeter are illustrated in Fig. 2. An OFHC copper cylinder 0.093 to 0.125 in. diam by about 0.40 in. long serves as the calorimeter case. A small (≈0.025 in. diam) flat bottom hole is drilled from the back end of the cylinder to within about 0.010 in. of the front surface. In most null-point calorimeters, a 0.020-in.-diam stainless steel thermocouple wire is used as the temperature sensor. The thermocouple type is ANSI Type K (Chromel®-Alumel) and the thermoelements are #38 AWG (0.004 in. diam). Attachment of the individual thermocouple wires in the bottom of the null-point cavity is normally done by vacuum brazing. The braze alloy generally used is NIORO which melts at 1,750°F and is composed of 82-percent gold (Au) and 18-percent nickel (Ni). To avoid altering the operating characteristics of the null-point calorimeter, a very small amount of braze alloy must be used.

Actual thermocouple wire attachment must be done in a vacuum oven/furnace because copper oxidizes at 750°F at atmospheric conditions. The inability to control the amount and location of the braze alloy is the primary reason that attachment of the thermocouple by brazing has proved to be an unreliable method.

A null-point calorimeter fabrication method developed by Calspan/AEDC personnel yields a high degree (80%) of reliability at a fraction (25%) of the cost of commercial units. All sensor components are shown in Fig. 2. A significant exception to methods used by commercial suppliers is that no braze is used in the fabrication process. Instead, the thermocouple lead wires are attached to the copper null-point body by a thermal fusion process using a miniature oxyacetylene torch. Another important advantage is gained by Calspan instrument technicians fabricating null-point calorimeters at the AEDC. Since there is ready access to an experimental calibration/characterization system, each null-point sensor can be experimentally checked for time response and output (calibration) at different points in the fabrication process. For instance, a unit which exhibits a slow time response can be brought well within acceptable tolerance by merely machining a few thousandths of an inch off the sensing surface.

COAXIAL SURFACE THERMOCOUPLE

In-house fabrication of coaxial surface thermocouples is not advised, especially for high-temperature operation. Fabrication of high-quality sensors requires specialized equipment and experience. Medtherm Corp. of Huntsville, AL, which is the only reliable source of coaxial thermocouples known to the author, allows the customer to effectively design his own sensor. Calspan/AEDC is currently using a standard size coaxial sensor with a body diameter of 0.0607 in. and length of 0.4 in. which is press fitted into the model/test article surface.

EXPERIMENTAL CONSIDERATIONS

Although the definition of transient temperature values and/or heat conduction patterns in the null-point calorimeter and coaxial surface thermocouple sensors by analytical means is of considerable interest to the designers/users of these devices, more significant progress has been made in the experimental areas. Because of manufacturers' inability to hold close tolerances in the fabrication of null-point calorimeters, a laboratory experimental characterization/calibration of each sensor before use in an arc facility measurement application is almost essential. Due to the harsh arc facility environment which occasionally causes damage to the sensor during a facility run, it is advantageous to be able to conduct an *in situ* experimental qualification of the sensor between runs. Time response and sensitivity are the two most important performance parameters to be experimentally evaluated. Recent advances in experimental methods at the AEDC enable these functions to be performed on a routine basis. These experimental methods and a limited quantity of data obtained with these techniques are described.

EQUIPMENT AND APPARATUS

Laboratory Data Acquisition and Processing System — A schematic block diagram and a drawing of the laboratory data acquisition and processing system used to obtain and reduce the transient experimental data are shown in Figs. 12 and 13, respectively. Since the date of last reporting,[4] a new front-end system, a 24-channel Preston GMAD3A-15B multiplexed analog-to-digital converter, has been incorporated into the laboratory data acquisition equipment. The new data acquisition equipment provides higher gains, higher resolution, higher signal-to-noise ratios, and better stability than the old system. Other system components include a DEC PDP-11/73 computer system, two DEC RL02 disk drives, a MDB MLSI-DWQ11 bus interpreter, a DEC UNIBUS expander box, DEC VT220 and VT240 display terminals, and a DEC LA50 printer/plotter. With the incorporation of the new data acquisition equipment, new user-friendly, menu-driven software has been written which establishes the AEDC calibration laboratory as a very versatile high-accuracy unit designed to perform a multiplicity of tasks. Ordinarily, when it is used to obtain sensor time response or calibration data at high heat-flux levels (>1,000 Btu/ft^2 -sec), the system is configured to accept data from four analog channels, at least one of which is routed through a thermocouple reference junction. These data are sampled at rates up to 0.2-msec intervals. The data acquisition system is synchronized with a high-speed shuttering system (described in following section) when obtaining time response data. Processed data in engineering units are available in hard copy tabular format or timewise plots in less than 5 min after the data are obtained.

High-Level Heat Source — Arc-heater facility stagnation heat flux can reach 25,000 Btu/ft^2-sec (28.4 kW/cm^2) at extreme test conditions; however, the majority of tests are conducted at heat-flux levels considerably lower. A high-level heat-flux source is needed to simulate actual arc facility test conditions in the laboratory. A goal for the laboratory heat source was to produce a heat flux high enough to approximate the medium to lower arc-heater levels.

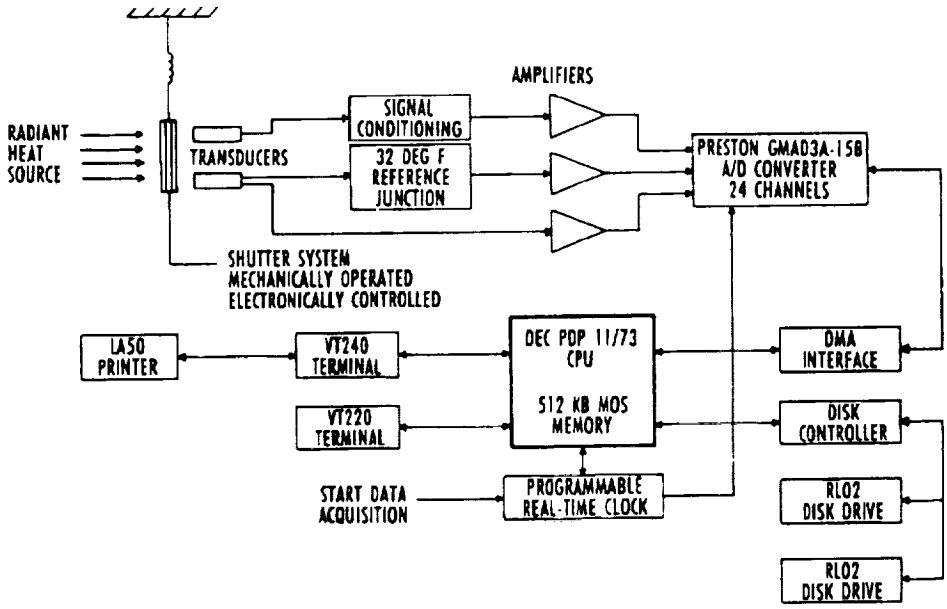

Fig. 12. Data acquisition/processing system block diagram.

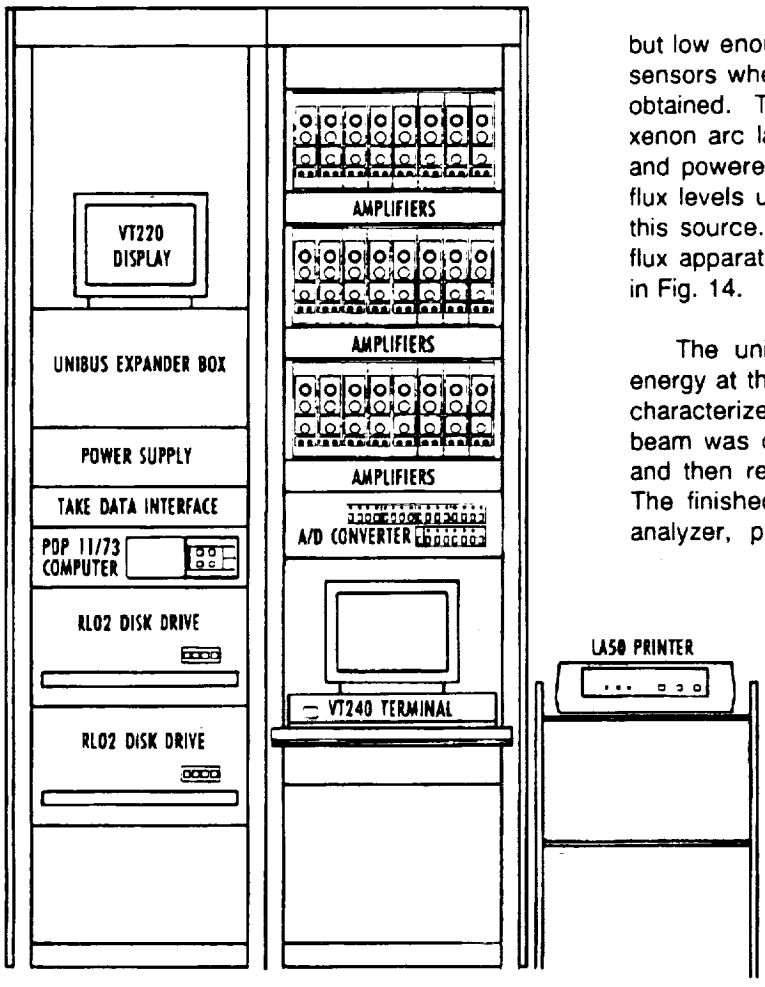

Fig. 13. Pictorial Drawing of thermal measurements laboratory data acquisition system.

but low enough to prevent damaging (by ablation) the sensors when time response and calibration data are obtained. This was accomplished with a 1.6-kW xenon arc lamp focused onto a relatively small area and powered by a pulsed 6-kW power supply. Heat-flux levels up to 2,500 Btu/ft^2-sec are attainable with this source. A block diagram of the entire high heat-flux apparatus, including support hardware, is shown in Fig. 14.

The uniformity of the focused beam of radiant energy at the focal plane of the arc lamp system was characterized by a photographic technique. The beam was directed onto a scatter plate of mill glass and then reimaged onto film with a pinhole camera. The finished photograph was digitized on an image analyzer, producing a digitized map of normalized radiant intensity as shown by the top two curves on Fig. 15. Pixel-to-pixel resolution was 0.005 in. on the X axis and 0.0061 in. on the Y axis.

Uniformity of the radiant intensity at the focal plane of the arc lamp as shown by the top curves on Fig. 15 was considered unacceptable for performing sensor calibrations with the high heat-flux source. Therefore, it was necessary to develop a method for achieving a better spot size uniformity. This need was met with the effective utilization of a simple optical integrator. The integrator was an aluminum tube with a highly polished inside surface

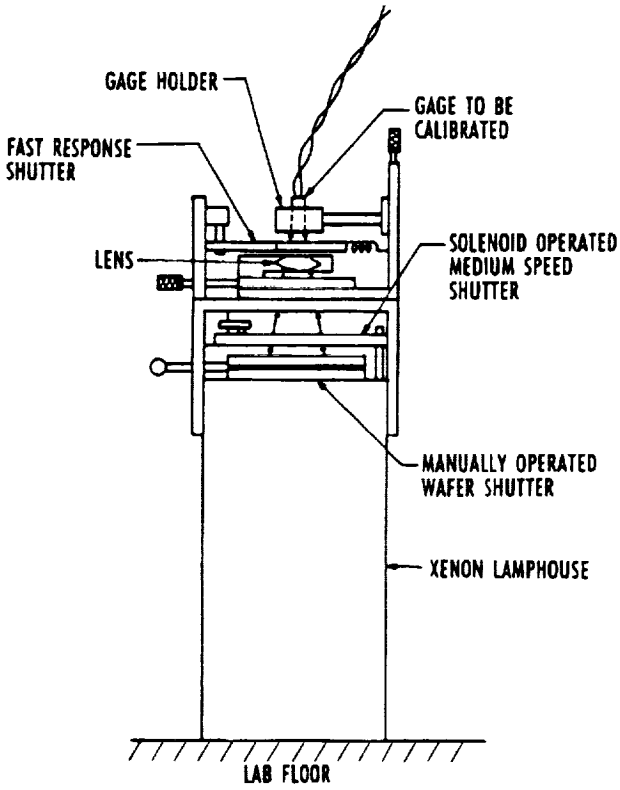

Fig. 14. Block diagram of high heat-flux system.

whose entrance was placed at the focal plane of the calibrator. Plots of the relative intensity in the X and Y axes at the exit plane of the tube are shown on the bottom curves on Fig. 15. As seen from Fig. 15, the magnitude of the radiant heat flux at the exit of the optical integrator is only about 65 percent of the intensity at the focal plane of the lamp system. A computer generated three-dimensional contour map of this intensity obtained with the digitized data from the image analyzer is shown in Fig. 16.

Shuttering System — A method of shuttering the high-level radiant heat source was devised to enable the equipment to perform the experimental calibration and time response functions. Three mechanically operated and electronically controlled shutters are used to expose the sensor to the heat source very quickly, but allow the heat source to irradiate the sensor long enough to obtain calibration data. The speed of the high-speed shutter has been experimentally determined to be about 200 in./sec. The fast shutter and the apparatus used to measure the speed are schematically illustrated in Fig. 17. Basically, the shutter consists of a spring-loaded plate with a slot large enough to completely expose the sensor to the heat

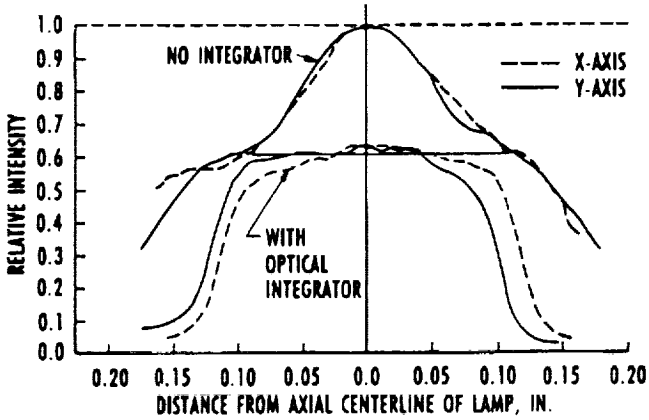

Fig. 15. Uniformity map of high heat-flux source on plane surface at focal point.

source. A 0.5-in.-diam copper sleeve houses a null-point or coaxial thermocouple sensor in the center and two fast response photodiodes whose axial centerlines are located 0.40 in. apart. Sleeves with small (0.013 in. diam) apertures are positioned above both photodiodes. Thus, the leading edge of the shutter opening will completely pass over the heat-flux sensor in less than 0.5 msec. This fast shutter is mechanically stopped with the slot completely open to the sensor. The sensor is shut off from the heat source when the second or middle shutter closes after being open for a time period which can be varied from 100 to 300 msec. Since the analytical data show that the time response of the fastest null-point calorimeter is about 1 msec to 95-percent of full-scale output, the shutter speed is easily fast enough to permit accurate sensor time response measurements.

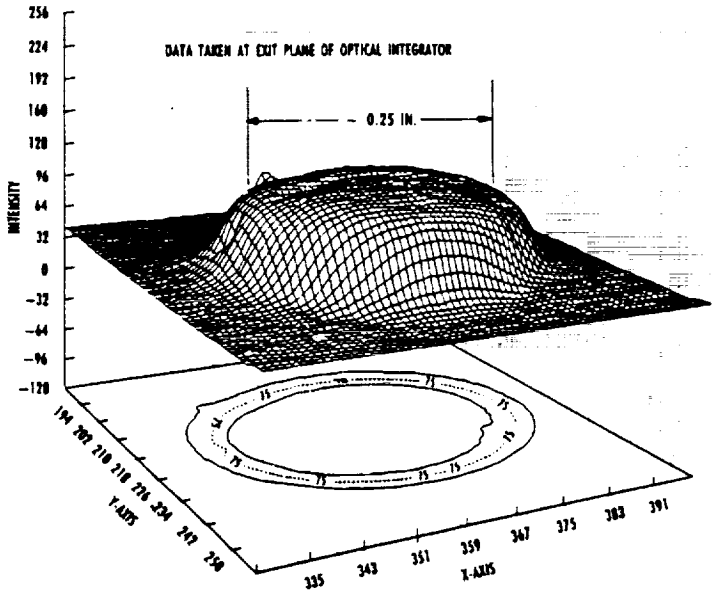

Fig. 16. Three-dimensional intensity map of arc lamp.

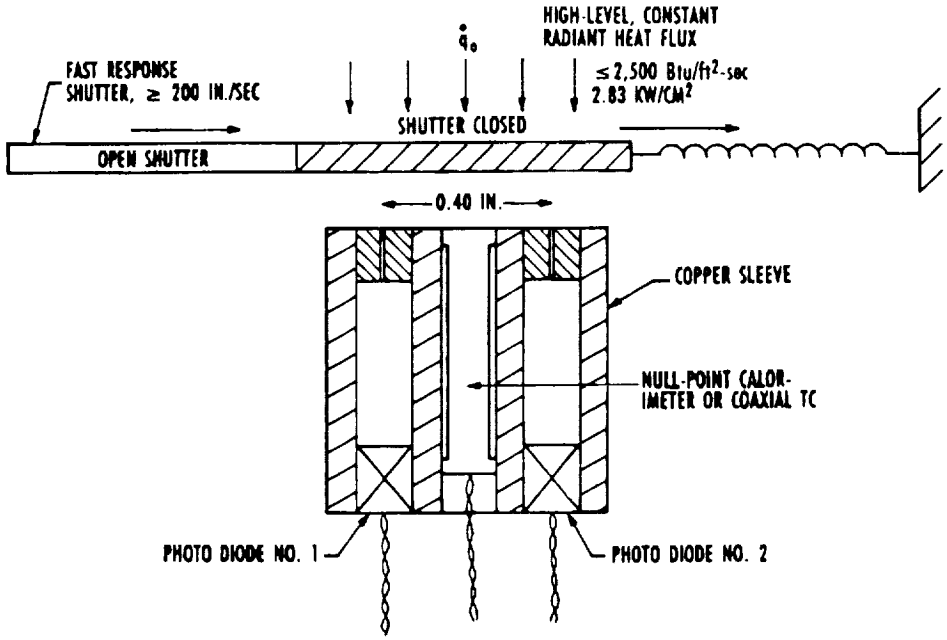

Fig. 17. Calspan/AEDC high heat-flux calibration and time response laboratory hardware.

Standards — Two commercial Gardon-type transducers were purchased and adapted to use as standards in the Calspan/AEDC high heat-flux calibration system. These transducers can be operated continuously with water cooling at heat-flux levels as high as 1,000 Btu/ft^2-sec (1.135 KW/cm^2). Since these transducers are irradiated for time periods of less than 0.5 sec, water cooling is not necessary. Certified traceability to the National Institute of Standards and Technology (NIST) is accomplished by calibration against a working standard which is calibrated against a transfer radiometer. The transfer standard radiometer is calibrated against a blackbody source whose temperature is measured with an optical pyrometer certified by NIST through application of the Stefan-Boltzmann equation.[15]

High Absorptivity Sensor Coating — A thin (<0.0005 in.) coating of high absorptivity must be applied to the sensing surface of each transducer and standard alike to perform accurate heat-flux transducer calibrations. This coating must be capable of withstanding relatively high temperatures (>1,000° F) in this transient measurement application. After screening several candidate coatings, Krylon® High Heat Spray Paint #611250 was chosen as the standard coating in this application because of the ease of application, high temperature capability, high absorptivity, and availability.

APPLICATIONS

A prevailing misconception regarding null-point calorimeters is that it is not possible to determine the actual time response of the sensors in the laboratory. Commercial suppliers of null-point calorimeters are presently unable to supply time response data with their sensors. Methods for obtaining null-point calorimeter experimental time response data have been developed for use at the AEDC. The experimental data generally complement the analytical data, thereby enhancing the credibility of both methods.

Since the construction of the high heat-flux source, the installation of the fast response shutter, and the integration of the data acquisition and processing system, literally hundreds of runs have been made to experimentally determine the time response characteristics and calibrations of null-point calorimeters and coaxial surface thermocouples. Some of these runs were made at the maximum attainable heat-flux level (≈ 2,500 Btu/ft^2-sec) of the heat source in its present configuration, but most were made at levels around 1,100 Btu/ft^2-sec. The data selected for presentation are intended to accentuate the more important aspects of the experimental system, rather than inundate the reader with large quantities of repetitious data. Some of the graphically illustrated data from different sensors are in poor agreement. These data are intentionally shown in this manner to show the poor quality control of some

commercial sensors and the ability of the laboratory experimental methods developed at the AEDC to detect the "bad" sensors before they are installed and used in test programs.

EXPERIMENTAL DATA

Experimental Characterization Data — To illustrate the full extent of the problem which exists with unqualified commercial null-point calorimeters, the experimental data shown on Fig. 18 are offered as an example. These data were obtained from several sensors using the high heat-flux source in 1988, before system upgrades such as fast shuttering, data acquisition and processing improvements, and high heat-flux standards were made. Null-point sensors were intentionally selected to show the large variations which may exist in commercial units. These sensors were not irradiated simultaneously, but rather consecutively on the same day within a 1-hr time period. Indicated heat-flux data should be in good agreement since the heat source has been shown to be quite stable over short (1 to 2 hr) time periods. The solid line represents transient indicated heat-flux data from a null-point sensor installed at the stagnation position of a copper sphere cone model (S/N:0.5-1-17) that was generally accepted as a standard against which other sensors were compared. The other three curves represent data acquired from sensors obtained in 1987 from the same commercial source in a group of about 75 units. Data obtained from sensor designated NPC-042 are in very good agreement with the data from the sensor in the probe model. However, data obtained from null-point calorimeters NPC-047 and NPC-111 are obviously unacceptable.

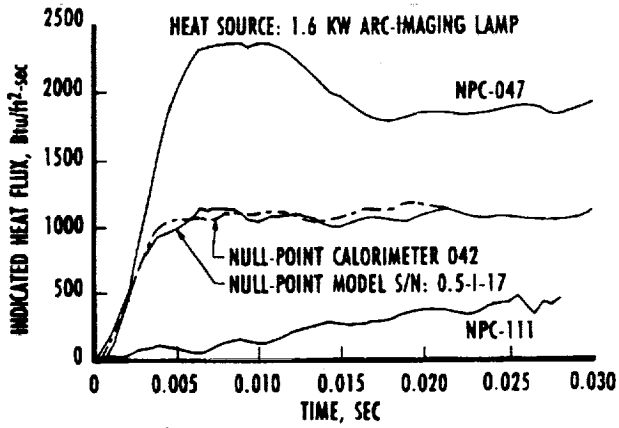

Fig. 18. Null-point calorimeter experimental characterization data.

The sluggish behavior of NPC-111 is caused by either a large quantity of braze in the null-point cavity, or a thermocouple wire attachment being made near or partially onto the cavity wall. Both problems will cause the sensor to exhibit slow response time and low output. In later years some sensors which exhibited strange behavior have been taken to the X-ray lab at the AEDC to be photographed. Careful examination of the photographs revealed the condition(s) referred to above. X-raying all sensors on a routine basis is time consuming, generally inconclusive, and therefore not cost effective. The transient behavior of NPC-111 is not typical, but has been experienced on a small number ($\approx$ 5 percent) of commercial units. This raises serious doubts about quality control procedures of commercial suppliers.

Analyzing the transient behavior of NPC-047 is more difficult, but a rational explanation does exist. What fabrication feature causes a sensor to initially indicate a heat-flux level more than twice the input level and then decrease to a constant level still well above this level? The only plausible reason is contained in the Analysis section of this documentation and is graphically illustrated by the top curves on Figs. 4 and 5. A reasonable explanation of the behavior of NPC-047 is that the thickness of the copper foil above the null-point cavity is significantly less than the design dimension. This effect is rare and only occurred on one other sensor out of a group of 75 units purchased from this supplier. After Calspan personnel at AEDC perfected the fabrication method now used, several units were intentionally made with a thin foil above the null-point cavity. This same type of behavior was seen in laboratory tests of these units. The data shown on Fig. 18 accentuate the necessity of getting better quality control from the commercial suppliers and performing laboratory experimental tests before wind tunnel use.

Experimental Time Response Data — It was accurately stated in earlier sections of this documentation that proper time response is critical for the accurate use of null-point calorimeters in arc facility heat-flux measurement applications. It was shown in the Thermal Analysis and Experimental Considerations sections that null-point calorimeters can respond too quickly, thus indicating a significantly higher level than the actual heat flux incident upon the instrument's sensing surface. And, of course, null-point sensors can easily be too slow for the intended application. Therefore, the capability of performing experimental time response characterizations at high heat-flux levels in the laboratory is of vital importance. The apparatus used at the AEDC for determining time response characteristics of heat-flux sensors was described in an earlier section of this paper. This section will show results of experimental time response characterizations of null-point calorimeters and coaxial surface thermocouples.

Figure 19 shows graphical illustrations of recent experimental time response data obtained from a Calspan/AEDC fabricated null-point sensor. These data were generated by irradiating a single null-point sensor with a high level (≈1,700 Btu/ft^2-sec) constant heat flux from the xenon arc lamp very quickly with the fast shutter and recording the timewise output at 0.2-msec time intervals. The timewise output was converted to a temperature history by applying the fifth-order equations for a Chromel-Alumel thermocouple. As shown on Fig. 19, the null-point cavity temperature increased by nearly 175° F in less than 30 msec. The resulting timewise heat flux on Fig. 19 was obtained by inserting the temperature history into Eq. (1) and applying the room temperature thermal properties of OFHC copper. A time response of 3 to 4 msec is indicated by the timewise heat-flux data. These data represent near optimum sensor behavior. If the copper foil above the null-point cavity was thinner, an operating behavior such as exhibited by NPC-047 in Fig. 18 probably would have resulted. This sensor will be installed at the stagnation position of a high-enthalpy probe model for AEDC arc facility measurement applications. After installation in the probe, the sensor will again be experimentally checked for time response and absolute calibration.

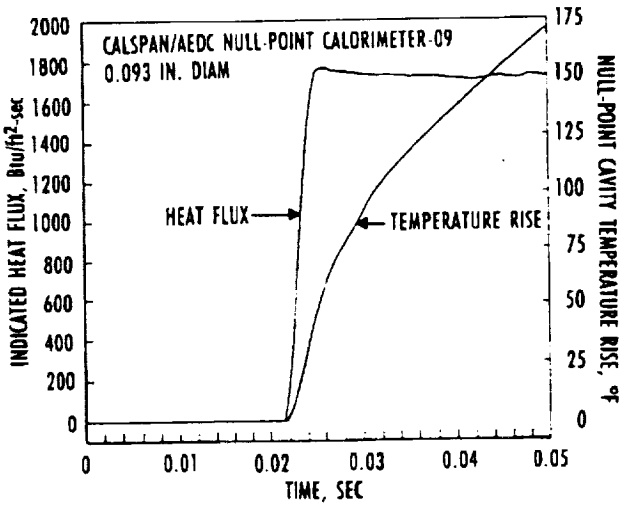

Fig. 19. Null-point calorimeter experimental time response data.

Time response data for a Chromel-constantan coaxial surface thermocouple are shown in Fig. 20 along with output signals from two photodiodes located 0.40 in. apart on either side of the coax TC as shown in Fig. 17. The output signals from the photodiodes indicate the speed of the fast response shutter. The time response of the coaxial sensor is shown to be about 2 msec. Since coaxial TC's have been shown to respond in about 50 µsec, the indicated time response is probably a result of the response of the data system and the numerical integration technique. It requires about five data points from a perfect temperature history to give an accurate indication of heat flux. Since the raw output data were sampled at 0.2-msec intervals, this accounts for about 1 msec. Normally, it is not necessary to perform time response characterizations on coaxial surface thermocouples for arc facility measurement applications. These data were presented to show the capabilities of the calibration system.

Absolute Calibration Data - Common practice at most high heat-flux test facilities worldwide is that null-point calorimeters and coaxial surface thermocouples are used without performing absolute calibrations against high heat-flux standards. The justification for this mode of operation is that neither the null-point calorimeter nor the coaxial surface thermocouple are actually heat-flux transducers/gages in the common use of the terminology. These sensors do

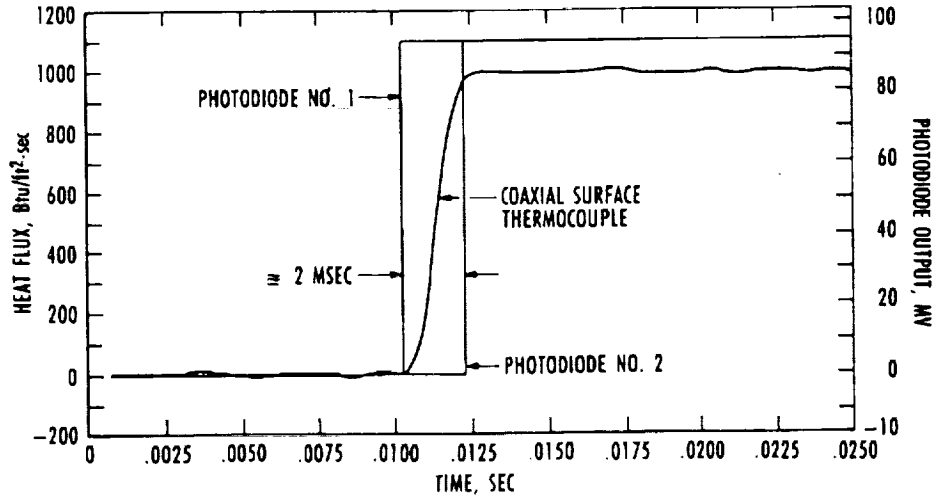

Fig. 20. High heat-flux calibrator time response data.

not provide an output signal directly proportional to the heat flux incident upon the sensing surface. They do provide timewise output signals from common thermocouples which can be accurately processed (converted) into the sensing surface temperature histories. Assuming the sensor behaves as a semi-infinite solid during the time period of interest, the temperature history is input to the numerically represented inverse heat conduction equation [previously shown as Eq. (1)] to obtain transient heat-flux data. Also required for obtaining accurate heat-flux data is a knowledge of the lumped thermal property parameter, $(\rho C_p K)^{1/2}$, previously defined in the Analysis section of this documentation. Thermal properties of OFHC copper are known to good accuracy up to temperatures approaching the melting point, 1,981° F. Although not as widely documented as copper, the $(\rho C_p K)^{1/2}$ parameter of both Chromel and constantan materials is well known from room temperature up to about 1,000°F. However, it is not a strong function of temperature.

If heat-flux measurement applications meet all the criteria outlined in the preceding paragraph, it would appear that absolute calibration of null-point calorimeters and coaxial surface thermocouples would not be necessary. However, results from the Analysis section of this paper show that the performance of null-point calorimeters is quite sensitive to dimensional variations. Therefore, it is advisable to calibrate all null-point calorimeters before installation and use in a facility test program. Conversely, the performance of coaxial surface thermocouples is historically quite stable. Occasional calibration of coaxial TC's can be helpful to check out the system.

Laboratory Experimental Calibration Data — A timewise comparison of indicated heat-flux data from two null-point calorimeters, a Chromel-constantan coaxial surface thermocouple, and one high heat-flux standard gage is shown on Fig. 21. These data were not obtained simultaneously, but rather in consecutive applications of the high-intensity radiant heat source. The calibration heat flux of about 600 Btu/ft^2-sec was intentionally set lower than maximum to stay within the calibration range of the standard gage. The three transient heat-flux sensors show relatively good agreement with the heat flux indicated by the Gardon type high flux standard. One of the null-point calorimeters was a stagnation sensor installed in a 0.5-in.-diam, 10-deg sphere-cone model. The other null-point calorimeter and the coaxial thermocouple were individual commercial units. Data from the standard gage are shown displaced on the time scale since the time response of the standard is about 50 msec. Because of the slower response of the standard gage and the fact that the output of the standard is directly proportional to the heat flux incident on the sensing surface, the timewise heat-flux indications from the standard do not contain the spurious noise spikes that are common with the fast response devices. Therefore, if the indicated heat flux is constant in time over a longer time span (0-300 msec), it is appropriate to apply this level over the entire shorter time period experienced in the laboratory calibration of the fast response sensors.

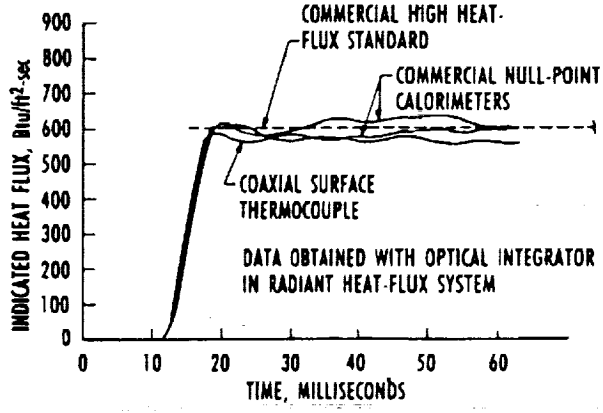

Fig. 21. High heat-flux transducer calibration data.

PORTABLE CALIBRATOR (*IN SITU* OPERATIONS)

Among the more significant recent achievements in arc facility heat-flux instrumentation at the AEDC is the capability to perform *in situ* calibrations of sensors in high-enthalpy probe models at the test site through the facility data acquisition system. This is accomplished by using a portable heat source system which can easily be moved in and out of the test area. This capability has greatly reduced the confusion and speculation with regard to anomalous heat-flux data from similar probes mounted on the same rake. Run-to-run heat-flux probe calibrations/characterizations can now be routinely performed without physically removing the probe from the facility structure (rake). The principal components of the system are a radiant heat source, a power supply, a shuttering mechanism, calibrator attachment hardware, and a standard gage holder.

HEAT SOURCE

Serving as the heat source for the portable calibrator is a 200-w tungsten filament lamp with a highly polished ellipsoidal reflector unit housed in a compact 2-in.-diam by 4.0-in.-long cylinder which focuses radiant energy onto a 0.30-in.-diam focal spot about 1 in. from the front end of the cylinder. A power supply which provides electrical power to the lamp from a common 120-VAC, 60-Hz source is included with the system which is a Model 4141 Mini-

Spot Heater manufactured by Research, Inc. A heat source adapter and a high-enthalpy probe holder shown in Fig. 22 were designed, fabricated, and are available for routine use in the calibration of null-point sensors in probes and/or individual sensors. A slot was milled in the probe holder (see Fig. 22) to permit shuttering the lamp and to provide transient data from the sensor. When taking calibration data through the facility data system, the system is actuated by a physical movement of the shutter. In its normal operational mode, the data system is configured to take 1,000 data points at 1-msec intervals. After the timing between the shutter and data acquisition system has been properly established, the number of calibration data points can be significantly reduced by a software change since accurate calibration data can be obtained from 100 to 150 data points.

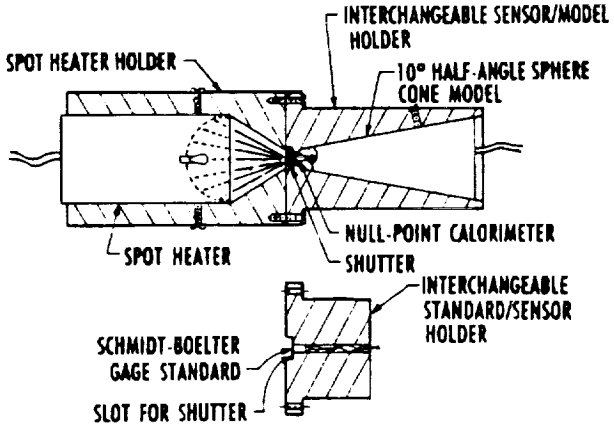

Fig. 22. Sketch of portable calibrator hardware.

An attachment which accommodates a heat-flux standard gage whose calibration is traceable to NIST[17] was designed to fit in exactly the same location (relative to the heat source) as the probe model in the probe holder attachment (see Fig. 22). Since the maximum rated incident heat flux which can be delivered to any surface with this source is only 123 Btu/ft^2-sec, a high-temperature Gardon gage[18] or a Schmidt-Boelter gage[19] can be used as the heat-flux standard.

APPLICATIONS

Graphical illustrations of the timewise heat flux measured by null-point calorimeters located at the stagnation position of two different 0.5-in.-diam, 10-deg half-angle sphere cone models on the same rake are shown on Fig. 23. These data were generated by the portable calibrator heat source on consecutive applications. Also shown is a dashed line which represents the heat-flux level indicated by a Schmidt-Boelter gage standard. The probe holder attachment was removed from the heat source hardware and the standard gage attachment was secured in its place. The output signal from the standard gage was converted to indicated heat flux by a simple direct multiplication of the output signal by the scale factor of the standard. Since the output from the standard gage was constant over a period of several seconds, the output signal can be recorded after the time response requirements of the gage ($\approx$1 sec) have been fully met. The measured heat-flux levels from the two probe models are in excellent agreement as well as with the indicated heat flux from the standard gage. Because of the relatively slow shutter speed with this portable source, time response data cannot be obtained with this device in its current configuration. Experimental data shown on Fig. 23 are in exceptionally good agreement. Often, probe models have to be discarded because of poor agreement with standard gages and/or good probes.

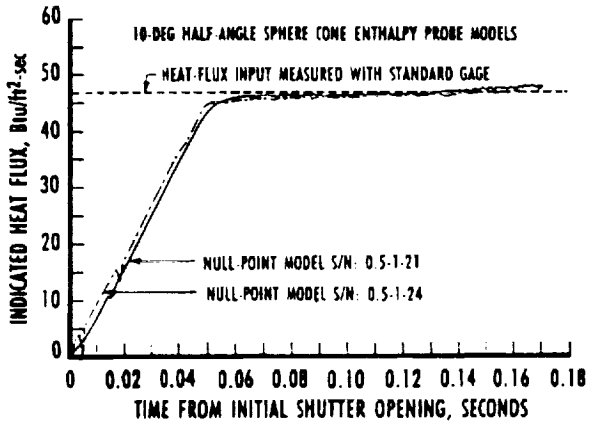

Fig. 23. Null-point calorimeter experimental data obtained with portable calibrator.

FACILITY DATA

The High Enthalpy Test Unit (HEAT) at the AEDC has two types of arc heaters.[20, 21] Both of these heat a continuous flow of high-pressure air to yield a high enthalpy test jet suitable for ablation testing of advanced nosetip materials and other high-pressure high heating rate tests. The arc heater at the AEDC which produces the highest flow-field enthalpies is of the segmented type and is designated H1.[21, 22] The segmented heater has 200 electrically isolated segments separating the anode (upstream) and cathode (nozzle end) of the heater. Air is injected at the upstream end and distributed through the individual segments to produce a uniform swirl, providing stability for the direct-current arc that heats the air.

Facility data include arc heater voltage and current, cooling water flow rate and temperature rise,

and air pressure and flow rate. These data define arc heater performance. Flow-field data, including heat-transfer rate measurements, are obtained with multiple standard probes that are swept through the flow field at speeds up to 90 in./sec. Flow-field data are nominally recorded at 5,000 points/sec with 1-kHz analog filters. Figure 24 is a graphical illustration of typical temperature and heat flux data obtained recently at the stagnation point of a 0.5-in.-diam, 10-deg half-angle sphere-cone standard probe in arc heater H1. The sensor was a 0.093-in.-diam copper null-point calorimeter fabricated by Calspan personnel at the AEDC. Although the null-point cavity temperature reached about 1,330° R during the run duration, it did not come close to the melting point of copper, which is 2,441° R (1,981°F). However, it should be noted that a coaxial surface thermocouple installed in a stainless steel model would have experienced surface ablation (and ultimate destruction) at this run condition.

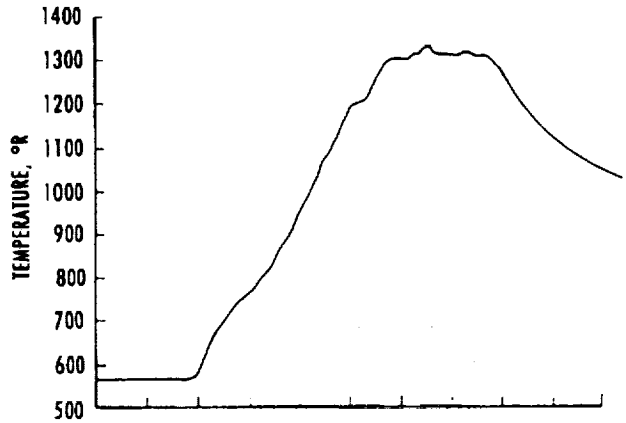

a. Timewise temperature

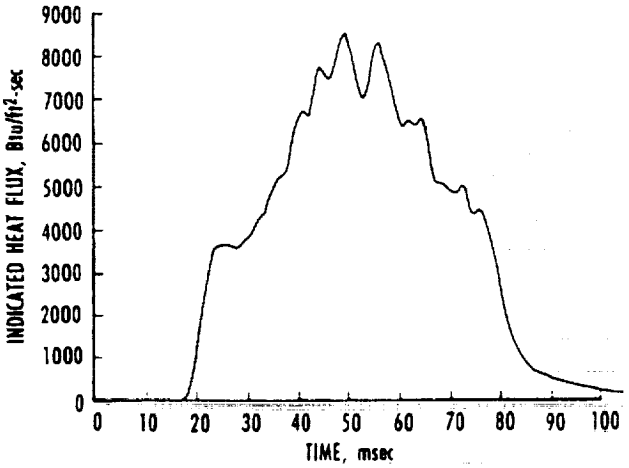

b. Timewise heat flux

Fig. 24. AEDC arc heater null-point probe data.

The null-point sensor was experimentally tested for time response and calibration in the high heat-flux calibration system (described in earlier sections of this paper) before and after installation in the standard copper probe. This sensor has set a durability record of sorts by surviving over 50 facility "runs" at last count with no apparent detrimental effects. Commercial probe/sensors historically have an inferior performance and survivability record.

CONCLUSIONS AND RECOMMENDATIONS

To improve the general quality of heat-flux data obtained in high-performance facilities at the AEDC, recent significant achievements have been made in several areas. Accomplishments to date and recommendations for future work are summarized below:

1. **Thermal Analysis** - Before 1990, analytical data which accurately defined the operation of the null-point calorimeter were virtually nonexistent in open literature. In Ref. 4 dated May 1990, the author published extensive analytical data obtained from a finite-element computer code which defined various aspects of null-point calorimeter behavior. Sensing that many users still have only a vague knowledge of the null-point calorimeter concept, some of the more important analytical data were reproduced and expanded upon in this document. Future null-point calorimeter design and fabrication should be influenced by analytical data presented in this paper.

In Ref. 8 also dated May 1990, the author published analytical data dealing with the coaxial surface thermocouple in transient heat-flux measurement applications. Although not as complex a measurement device as the null-point calorimeter, the constraints which apply to the coaxial TC in aerothermal measurement applications are still not well understood by many would-be users. This paper points out that the coaxial TC need not be restricted to semi-infinite solid time limitations.

2. **Fabrication** - It is stated in this document that null-point calorimeters are routinely fabricated by Calspan instrument technicians at the AEDC at a cost of about 25 percent that charged by commercial vendors with a success rate of about 80 percent per unit. This is accomplished by attaching the thermocouple wires in the null-point cavity by thermal fusion.

3. **Laboratory Experimental Methods** - Most suppliers and users of null-point calorimeters consider experimental time response and calibration data to be unattainable in the laboratory. Experi-

mental methods were devised and equipment was designed, fabricated, and assembled which enable these data to be obtained on a routine basis at heat-flux levels exceeding 2,000 Btu/ft^2-sec (2.27 kW/cm^2) in the Thermal Measurements Laboratory at the AEDC. Recent data acquisition and processing system upgrades now permit higher quality data to be supplied in a more timely and effective format. This unique (to the AEDC) experimental capability has proved to be most valuable in the calibration and characterization of new sensors and old sensors which have experienced the rigors of arc heater flow-field environments. Future upgrades of these experimental facilities are planned to meet the needs of NASP heat-flux instrumentation calibrations and characterizations.

4. **Portable Calibrator (*In Situ* Operation)** - A portable calibrator which can be transported to the test site to perform *in situ* calibrations of null-point calorimeters through the facility data acquisition/processing system has been developed and effectively used in the AEDC arc heater facilities. This portable heat source can be applied in the test area without removing heat-flux probes from the flow-field rake. This system has been most effective in minimizing the confusion and speculation with regard to transient heat-flux measurements on different probes on a test rake. Although the maximum heat flux which can be attained with this system at present is only 123 Btu/ft^2-sec, a significant accomplishment has been made in flow-field diagnostic probe qualification methods. It would be desirable to increase the available heat flux to about 1,000 Btu/ft^2-sec and install a high-speed shutter on the device to enable time response data to be obtained at the test site.

REFERENCES

1. Beck, J. V. and Hurwicz, H. "Effect of Thermocouple Cavity on Heat Sink Temperature." *Journal of Heat Transfer*, Vol. 82, No. 1, Feb. 1960, pp. 27-36.

2. Howey, D. C. and DiChristina, V. "Advanced Calorimetric Techniques for Arc Plasma Heat Transfer Diagnostics in the Heat Flux Range up to 20 KW/cm^2." AIAA Paper 68-404, San Francisco, CA, April 1968.

3. Kennedy, W. S., Rindal, R.A., and Powars, C.A.,"Heat Flux Measurements Using Swept Null Point Calorimetry." AIAA Paper 71-428, Tullahoma, TN, April 1971.

4. Kidd, C. T. "Recent Developments in High Heat-Flux Measurement Techniques at the AEDC." *Proceedings of the 36th International Instrumentation Symposium*, May, 1990, pp. 477-492.

5. Czysz, Paul and Kendall, David "Testing Technology Advances Associated With Development of an ARC Heated Impulse Tunnel." AIAA Paper No. 66-759, Los Angeles, CA, Sept. 21-23, 1966.

6. Trimmer, L. L., Matthews, R. K., and Buchanan, T.D. "Measurements of Aerodynamic Heat Rates at the AEDC von Karman Facility." International Congress on Instrumentation in Aerospace Simulation Facilities, September 1973.

7. Hedlund, E. R., Hill, J. A. F., Ragsdale, W. C., and Voisinet, R. L. P. "Heat Transfer Testing in the NSWC Hypervelocity Wind Tunnel Utilizing Co-Axial Surface Thermocouples." NSWC MP 80-151, March 1980.

8. Kidd, C. T. "Coaxial Surface Thermocouples: Analytical and Experimental Considerations for Aerothermal Heat-Flux Measurement Applications." *Proceedings of the 36th International Instrumentation Symposium*, May 1990, pp. 203-211.

9. Neumann, R. D. "Aerothermodynamic Instrumentation." AGARD Report No. 761, May 1988.

10. Starner, K. C. "Use of Thin-Skinned Calorimeters for High Heat Flux Arc Jet Measurements." ISA Preprint No. P-11-5 PHYMMID-67, presented at 22nd Annual ISA Conference and Exhibit, September 1967.

11. Standard Method for Measuring, "Extreme Heat-Transfer Rates from High-Energy Environments Using a Transient, Null-Point Calorimeter." ASTM Designation: E 598-77, 1977 (Reapproved 1990).

12. Marchand, E. O. "One-Dimensional, Transient Heat Conduction in Composite Solids." University of Tennessee Space Institute Master's Thesis, August 1974.

13. Rochelle, J. K. "TRAX - A Finite Element Computer Program for Transient Heat Conduction Analysis of Axisymmetric Bodies." University of Tennessee Space Institute Master's Thesis, June 1973.

14. Cook, W. J. and Felderman, E. J. "Reduction of Data from Thin-Film Heat-Transfer Gages:A Concise Numerical Technique." *AIAA Journal*, Vol. 4, Number 3, March 1966.

15. Carslaw, H. S., and Jaeger, J. C. *Conduction of Heat in Solids*. Clarendon Press, Oxford, 1959 (Second Edition).

16. Touloukian, Y. S., ed. "Thermophysical Properties of High Temperature Solid Materials, Volume 1: Elements." Thermophysical Properties Research Center, Purdue University, MacMillan Company, New York, 1967.

17. Kidd, C. T. "Determination of the Uncertainty of Experimental Heat-Flux Calibrations." AEDC-TR-83-13 (AD-A131918), August 1983.

18. Gardon, Robert "An Instrument for the Direct Measurement of Intense Thermal Radiation." *The Review of Scientific Instruments*, Vol. 24, May 1953, pp. 366-370.

19. Kidd, C. T. "A Durable, Intermediate Temperature, Direct Reading Heat-Flux Transducer for Measurements in Continuous Wind Tunnels." AEDC-TR-81-19 (AD-A107729), November 1981.

20. Smith, Richard T. and Folck, James L. "Operating Characteristics of a Multimegawatt Arc Heater Used With the Air Force Flight Dynamics Laboratory 50-Megawatt Facility," AFFDL-TR-69-6, Air Force Flight Dynamics Laboratory, Wright-Patterson Air Force Base, OH, April 1969.

21. Horn, D. D. and Smith, R. T. "AEDC High Enthalpy Ablation Test (HEAT) Facility Description, Development, and Calibration." AEDC-TR-81-10 (AD-A101747), July 1981.

22. Carver, D. B. and Kidd, C. T. "Heat-Transfer Measurement Uncertainty in Arc-Heated Flows." *Proceedings of the 37th International Instrumentation Symposium*, May 5-9, 1991, pp. 951-967.